

Electronic Supplementary Information

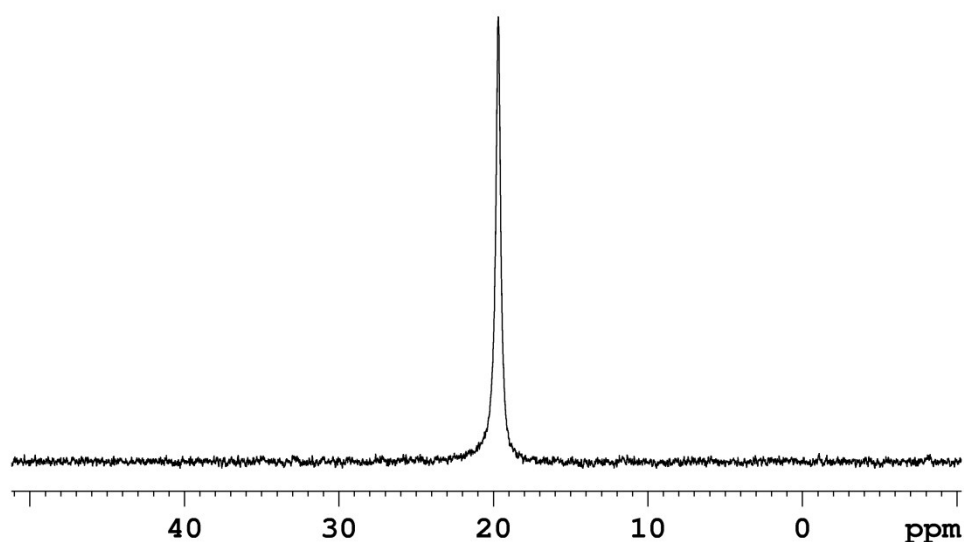


Figure S1.  $^{31}\text{P}$  NMR spectrum of PEG-Ner.

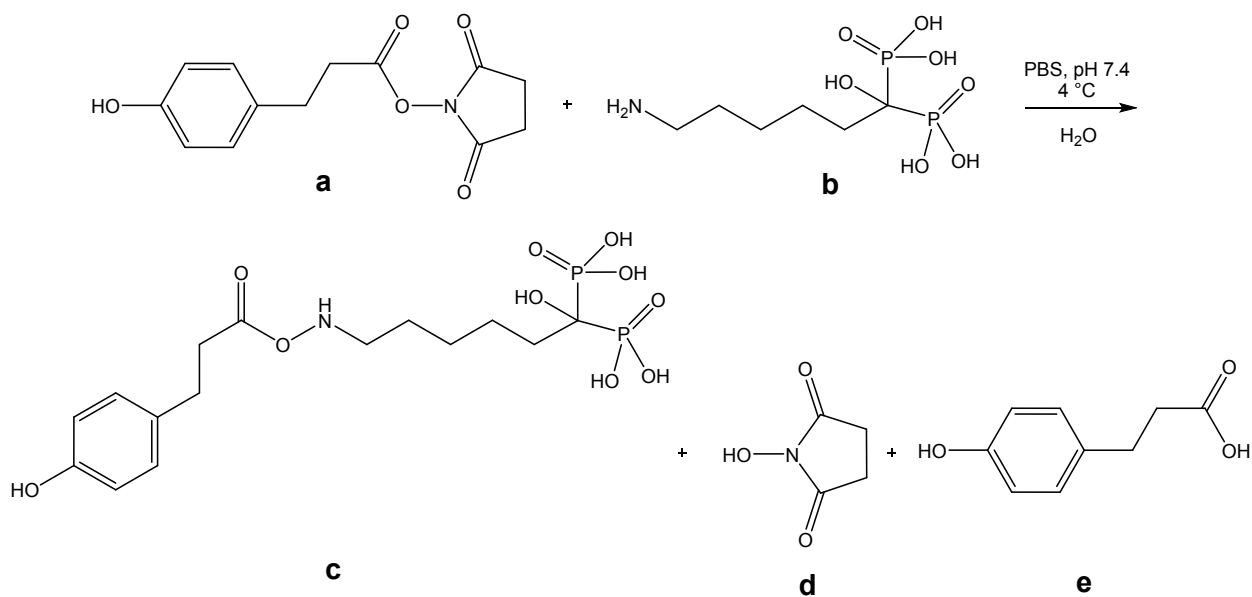
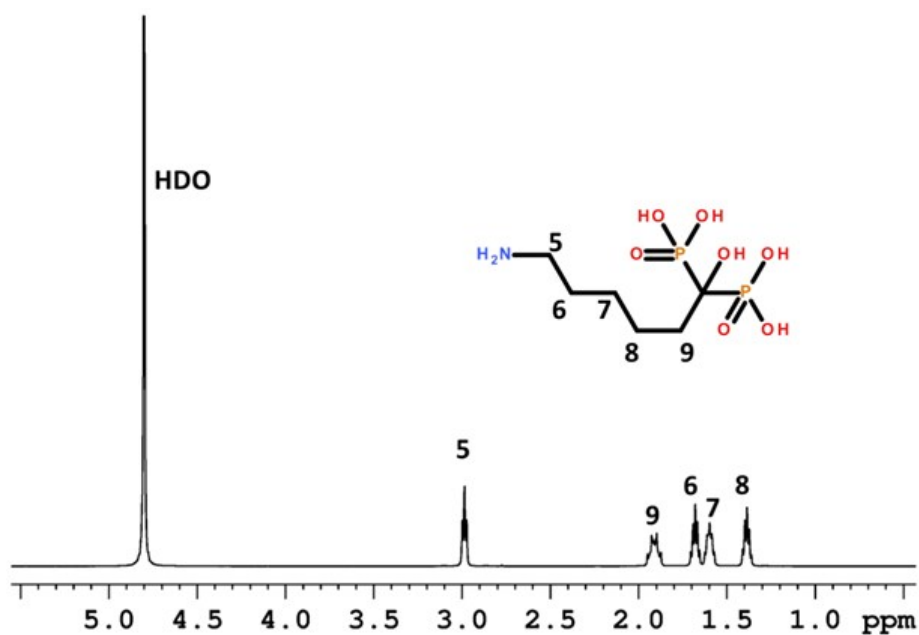
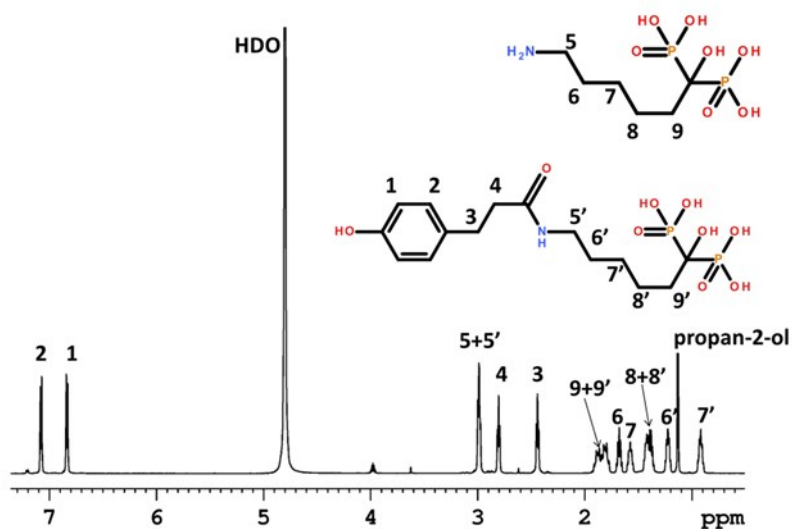


Figure S2. Scheme of synthesis and purification of BH-Ner. (c) BH-Ner, (d) *N*-hydroxysuccinimide, and (e) 3-(4-hydroxyphenyl)propanoic acid obtained by hydrolysis of (a) initial Bolton-Hunter reagent. Cold acetone or propan-2-ol was added to the reaction mixture, which was aged at 4 °C for 24 h. As a result, PBS formed large crystals, while (b) and (c) formed suspension, which was isolated by decantation. (b) and (c) were filtered-off from the suspension, washed with propan-2-ol three times, and dried; (d) and (e) products remained in solution.



**Figure S3.** <sup>1</sup>H NMR spectrum of sodium neridronate. Peaks assigned to five methylene groups were at 2.99 (t, 2H; CH<sub>2</sub>), 1.91 (m, 2H; CH<sub>2</sub>), 1.68 (t, 2H; CH<sub>2</sub>), 1.60 (m, 2H; CH<sub>2</sub>), and 1.39 ppm (m, 2H; CH<sub>2</sub>). The integrals of all five peaks were equal.



**Figure S4.** <sup>1</sup>H NMR spectrum of BH-Ner with admixture of sodium neridronate. All five peaks were attributed to methylene groups of sodium neridronate, but the integrals were not equal: 1.00 for (5), 0.45 for (6), 0.46 for (7), 1.04 for (8), and 1.03 for (9). Two additional peaks at 1.26 and 0.95 ppm had the integrals 0.58 and 0.57 respectively, which were complementary to the integrals of (6) and (7) giving in a pair a sum ~1. To find if extra peaks at 1.26 and 0.95 ppm belonged to the BH-Ner or to admixtures, the 2D <sup>1</sup>H NMR COSY spectrum was measured (Figure S5).

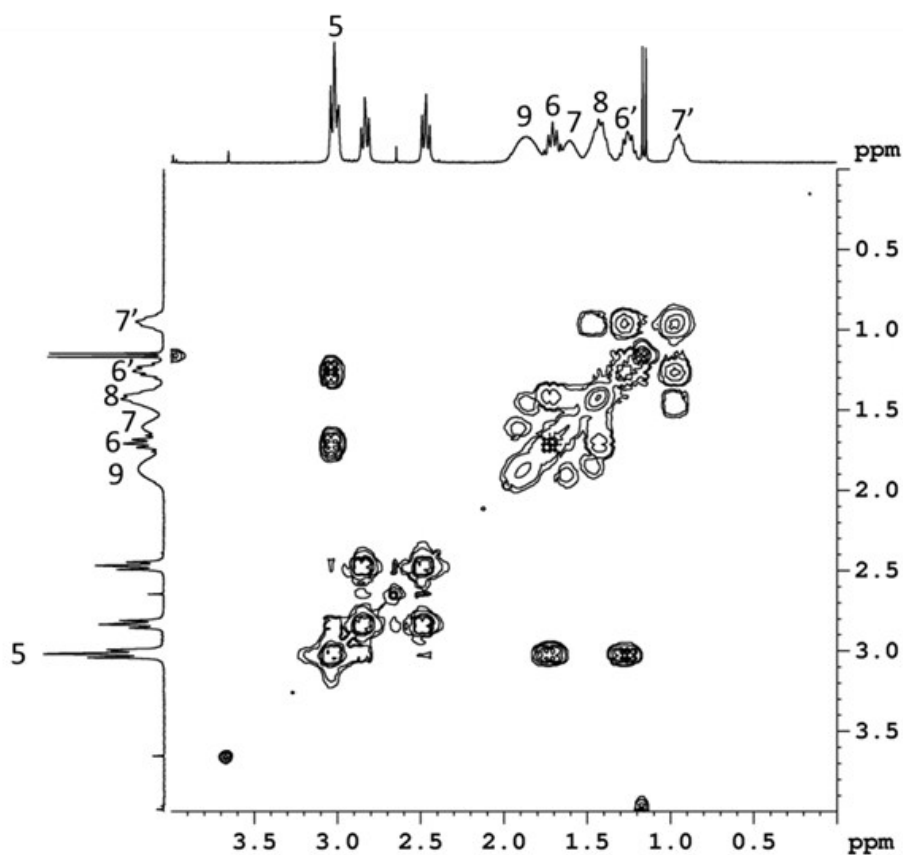


**Figure S5.** 2D <sup>1</sup>H NMR COSY spectrum of BH-Ner and sodium neridronate. Numbering of the peaks was similar as in Figures S3 and S4. Peak at 1.26 ppm was strongly correlated with methylene group (5) and the peak at 0.95 ppm. Similar correlations were observed for methylene group (6) and the peak at 1.26 ppm was assigned as (6'). The peak at 0.95 ppm was correlated with methylene group (8) and the peak (6'). Similar correlations were found for methylene group (7) and the peak at 0.95 ppm was assigned as (7'). Two additional peaks at 1.26 and 0.95 ppm belonged to the methylene groups in neridronate. No correlation was observed between (6) and (6'), as well as between (7) and (7'), confirming that they belonged to different molecules. Since the integrals of (6') and (7') were equal to the integrals of methylene groups (3) and (4), as well as to the integrals of Ar (1) and (2) in Bolton-Hunter group (Figure S4), it was assumed that peaks (6') and (7') belonged to the BH-Ner product. Peaks of methylene groups (5'-9') in BH-Ner were shifted compared to sodium neridronate peaks (5-9): 2.99 (m, 2H; CH<sub>2</sub>) - (5+5'), 1.91 (m, 2H; CH<sub>2</sub>) - (9+9'), 1.68 (t, 2H; CH<sub>2</sub>) - (6), 1.60 (m, 2H; CH<sub>2</sub>) - (7), 1.39 (m, 2H; CH<sub>2</sub>) - (8+8'), 1.26 (m, 2H; CH<sub>2</sub>) - (6'), and 0.95 ppm (m, 2H; CH<sub>2</sub>) - (7'). The ratio of integrals of methylene groups (3) or (4) in Bolton-Hunter group to the integral of methylene group (5+5') in neridronate was 1:1.6 (see Figure S4). Calculated substitution of sodium neridronate with Bolton-Hunter reagent was 62.5 mol.%. The product was used for interaction with the nanoparticles without further purification.

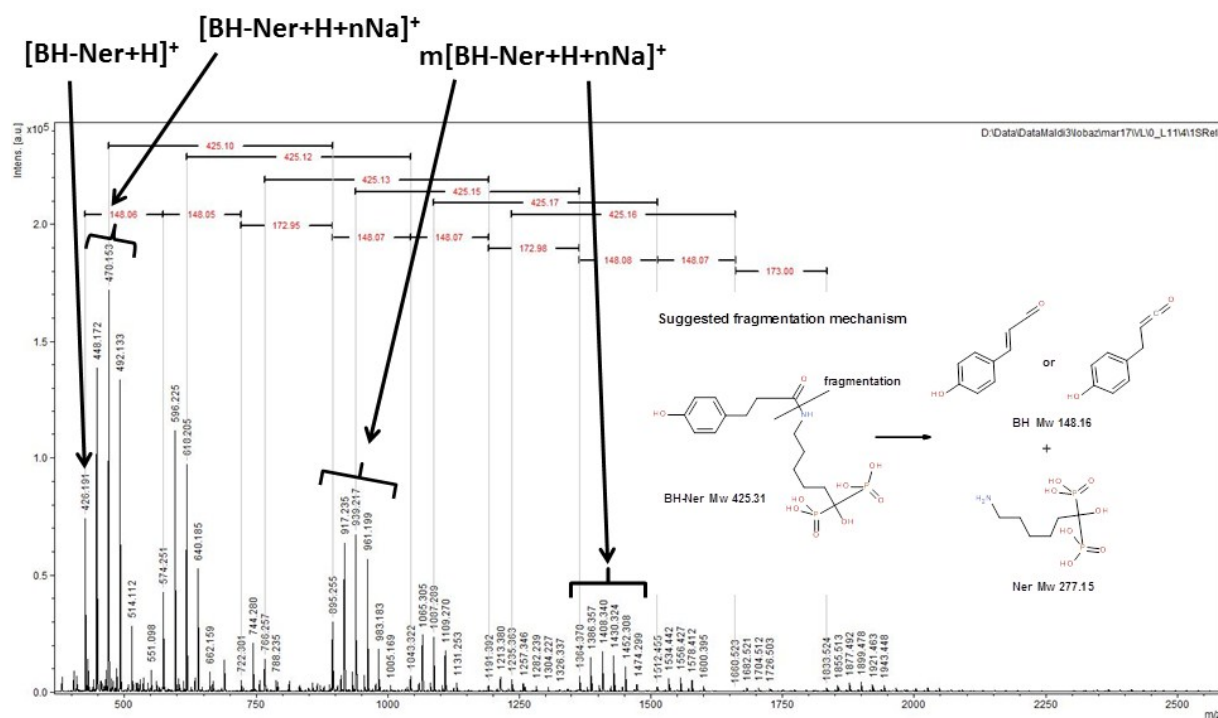


**Figure S6.** MALDI-TOF spectrum of BH-Ner in 2,5-dihydroxybenzoic acid matrix. Peak at 426.191 m/z was attributed to protonated [BH-Ner H]<sup>+</sup>. [BH-Ner+H+nNa]<sup>+</sup> - 448.172, 470.153, 492.133, and 514.112 m/z - were adducts of protonated BH-Ner with sodium ions, which replaced protons of hydroxybisphosphonate group. Other groups of peaks at higher m/z corresponded to adducts of m[BH-Ner+H+nNa]<sup>+</sup> ions and product of BH-Ner fragmentation at amide bond ( $M_w = 148.16$  g/mol). Sodium neridronate ( $M_w = 277.15$  g/mol), 2,5-dihydroxybenzoic acid ( $M_w = 154.12$  g/mol), and their adducts with sodium ions were not observed in the spectrum.

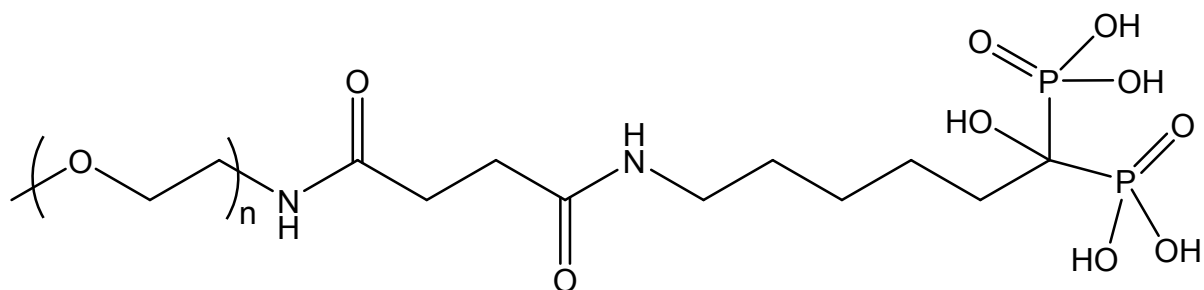


**Figure S7.** Chemical structure of PEG-neridronate.

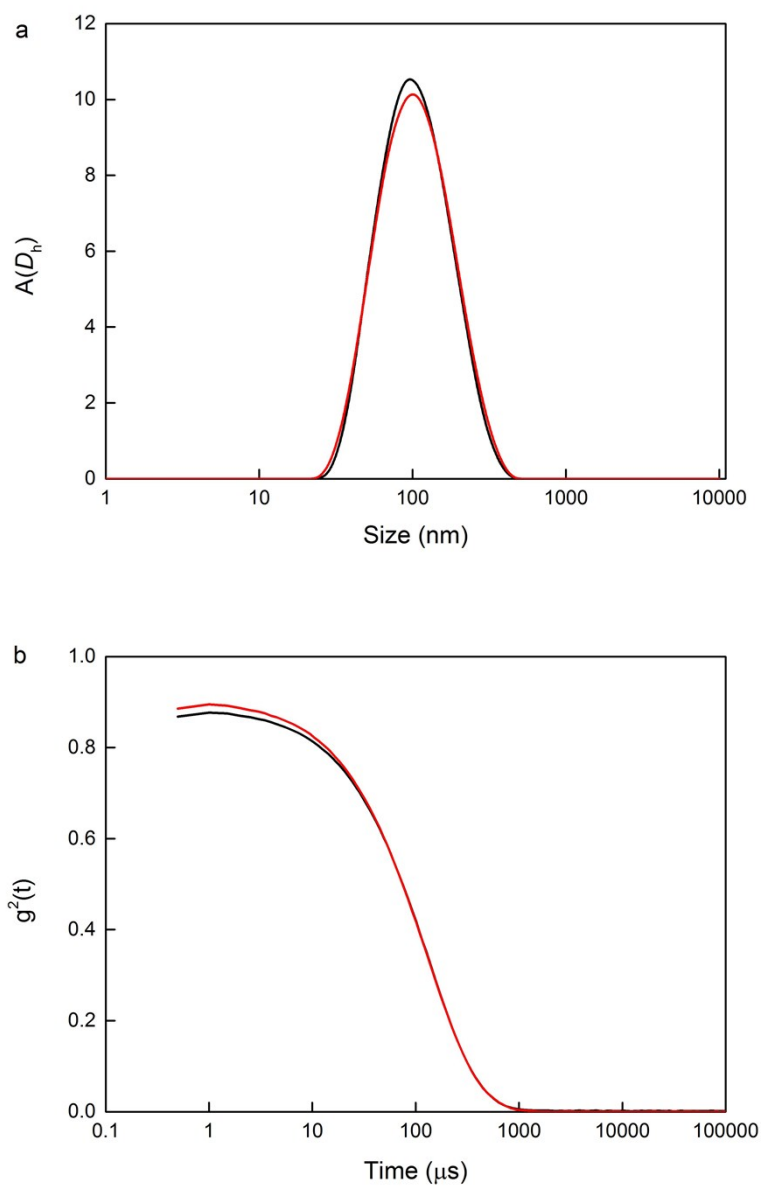


**Figure S8.** (a)  $\text{NaYF}_4:\text{Yb}^{3+}/\text{Er}^{3+}$ @PEG nanoparticle size distribution calculated from intensity-weighted distribution function  $A(D_h)$  and (b) autocorrelation decay plot  $g_2(t)$ . Dispersion of the particles in albumin-containing PBS was just prepared (black curve) and after 350 h (red curve).

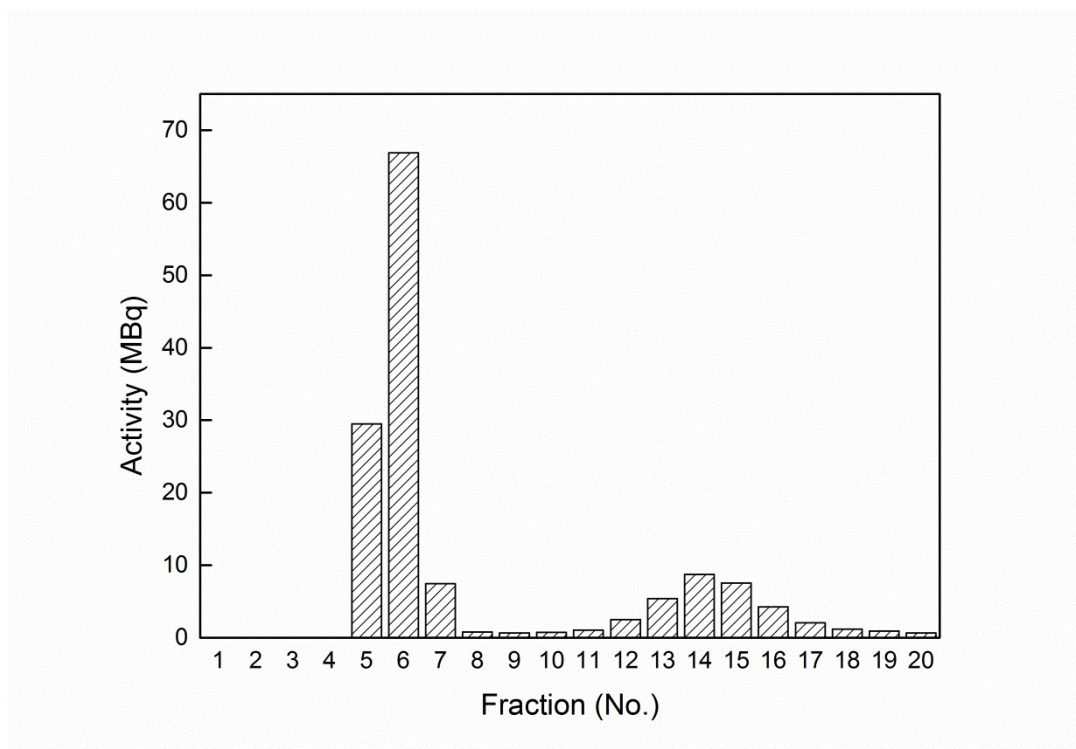


**Figure S9.** Radioactivity of  $^{125}\text{I}$ -labeled  $\text{NaYF}_4:\text{Yb}^{3+}/\text{Er}^{3+}@\text{PEG}$  nanoparticles and  $\text{Na}^{125}\text{I}$  fractions.

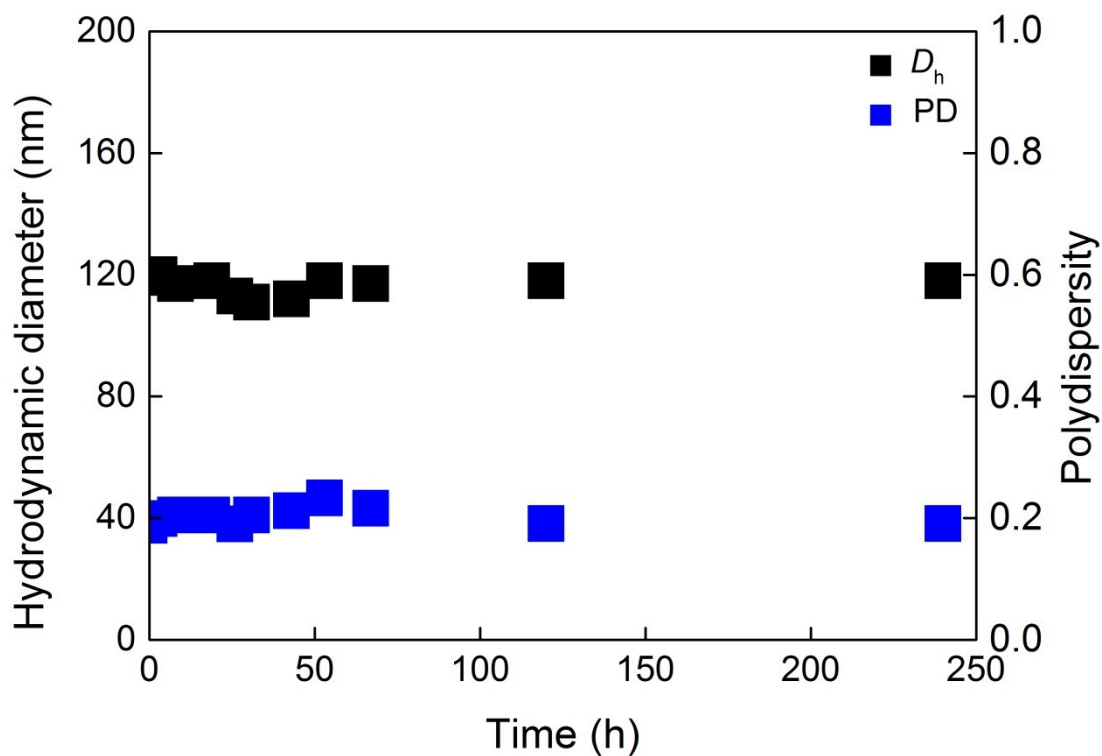


**Figure S10.** Hydrodynamic diameter  $D_h$  and polydispersity PD of  $^{125}\text{I}$ -labeled  $\text{NaYF}_4:\text{Yb}^{3+}/\text{Er}^{3+}@\text{PEG}$  nanoparticles in PBS.

Calculated average PEG footprint area from TGA results under the assumption of spherical particles ( $2.2 \text{ nm}^2$  per PEG-Ner ligand) corresponds to high-quality dense coating and is comparable to literature data on PEG coating of different particles.<sup>51</sup>

S1 J.V. Jokerst, T. Lobovkina, R.N. Zare, and S.S. Gambhir, *Nanomedicine*, 2011, **6**, 715.